

Voltammetric Determination of Ferulic Acid on Carbon Mesoporous Modified Glassy Carbon Electrode

AYUSHI SRIVASTAVA^{1,*} and SADHANA SHRIVASTAVA²

¹School of Studies in Chemistry, Jiwaji University, Gwalior-474001, India

²Department of Chemistry, Government S.L.P. (P.G) College, Morar, Gwalior-474006, India

*Corresponding author: E-mail: ayushi021993@gmail.com

Received: 28 November 2022;

Accepted: 10 January 2023;

Published online: 27 February 2023;

AJC-21149

The electrochemical determination of ferulic acid was carried out with highly sensitive and rapid square wave voltammetry (SWV) and cyclic voltammetry (CV) techniques by using bare glassy carbon electrode and carbon mesoporous fabricated glassy carbon electrode (CMP/GCE). The oxidation kinetics of ferulic acid was studied after the experimental conditions were optimized. A voltammetric study of ferulic acid at the CMP/GCE electrode exhibited a well-defined anodic peak in phosphate buffer at pH 2.2. The square wave oxidation peak current of ferulic acid was linearly increased over the concentration range from 1 to 7 $\mu\text{g mL}^{-1}$. The LOD and LOQ for ferulic acid were calculated as 0.36 and 1.10 $\mu\text{g mL}^{-1}$, respectively. The analytical application of the developed sensor was evaluated by a real sample analysis of ferulic acid in sweet corn.

Keywords: Ferulic acid, Square wave voltammetry, Cyclic voltammetry, Electrode sensor, Sweet corn.

INTRODUCTION

Ferulic acid (4-hydroxy-3-methoxy cinnamic acid) belongs to the phenolic acid group commonly found in plant tissues and exists in both *cis*- and *trans*-isomeric forms [1,2]. The *trans*-derivatives of ferulic acid have potential therapeutic applications as an antioxidant. It also possesses antithrombotic, anticancer, antineoplastic, antibacterial, hypolipidemic, antimicrobial and anti-inflammatory activities as well as it plays an important role in the clinical treatment of cardiovascular disorders and neurodegenerative disorders [3-14].

Ferulic acid shows antioxidant properties by its 3-methoxy and 4-hydroxyl groups attached to the benzene ring when reacting with the free radicals resulting in the formation of phenoxyl radical intermediate and terminating free radical chain reaction [15]. The phenoxyl radical intermediate stabilizes by the presence of carboxylic acid groups with unsaturated carbon-carbon double bond as well as it provides an additional attack site for free radicals [15]. Further, lipid peroxidation is prevented by the carboxylic acid group by facilitating ferulic acid to act like an anchor by binding to the membrane lipid bilayer [16].

Quantitative measurement of ferulic acid includes micellar electro-kinetic chromatography, HPLC, chemiluminescence, gas chromatography, ultraviolet-visible spectroscopy, thin layer chromatography, *etc.* [17-19]. Though these techniques are highly expensive, time taking and require pre-treatment steps. To overcome the disadvantages of these methods an electrochemical analysis shows the wide application prospects in the field of analysis of antioxidants due to its cheap, effective, highly sensitive and simple operation.

In present work, the electrochemical techniques such as square wave voltammetry and cyclic voltammetry have been used for the analysis of *trans*-ferulic acid with the help of bare glassy carbon electrodes and carbon mesoporous fabricated glassy carbon electrodes (CMP/GCE).

EXPERIMENTAL

trans-Ferulic acid and carbon mesoporous were purchased from Sigma-Aldrich, USA. Ferulic acid was used as received and suspension of carbon mesoporous was prepared in DMF. All the chemicals used were of analytical grade and the doubly distilled water was used throughout the experiment. The stock

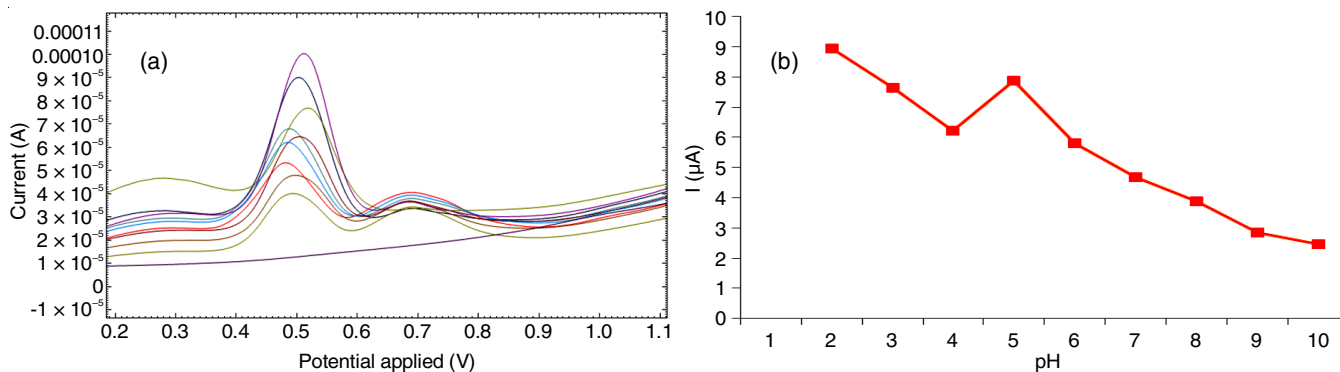


Fig. 1. (a) Square wave voltammogram of effect of pH on ferulic acid oxidation in phosphate buffer and (b) optimization of effect of pH

solution of ferulic acid (1 mg mL^{-1}) was prepared for the voltammetric measurements in methanol solvent.

Characterization: The voltammetric studies were carried out using a μ -AUTO LAB TYPE III (Eco-chemie B.V., Utrecht, The Netherlands) potentiostat-galvanostat with NOVA 1.10 computrace software. Carbon mesoporous modified glassy carbon electrode (CMP/GCE) was used as a working electrode, reference electrode as silver/silver chloride electrode (Ag/AgCl) and platinum wire or sheet was used as an auxiliary electrode. The pH measurements were carried out on the Decibel DB-1011 digital pH meter.

Preparation of carbon mesoporous modified glassy carbon electrode (CMP/GCE): Carbon mesoporous (CMP) suspension was prepared by adding 1 mg dissolved in DMF, followed by ultrasonication for 2 h to obtain a homogenous suspension. A glassy carbon electrode (GCE) was prepared for modification by washing with double distilled water and subsequently polishing its surface with alumina (Al_2O_3) powder (particle size ranges from $0.05 \mu\text{m}$ to $0.1 \mu\text{m}$) on a micro cloth pad, an electrode was further rinsed thoroughly with a Milli Q water and ultrasonication was performed for 10-20 min to remove any adsorbed impurities. Further, GCE was dried at room temperature, this process was repeated until the mirror-like finish was obtained. When homogeneous CMP suspension was obtained, a known volume of $10 \mu\text{L}$ of suspension was cast onto the cleaned surface of the glassy carbon electrode. The modified CMP/GCE electrode was then placed at room temperature in a desiccator for drying.

Preparation of real samples: Sweet corn was purchased from the market, washed with double distilled water, dried and then crushed with the help of a mixer grinder. Crushed samples were refluxed successively with aqueous ethanol (5%, 100 mL) for 8 h and then vapours were condensed under cool running water and collected back into the flask. The extracts were filtered through Whatman filter paper and centrifuged at 4000 rpm for 10 min, collected and then stored at 4°C in a refrigerator for further analysis.

RESULTS AND DISCUSSION

Optimization of experimental parameters

Effect of pH: The effect of various buffer solutions (phosphate buffer and Britton-Robinson buffer) and their different

pH were employed to investigate the current response of ferulic acid. Buffer ranges from 2.2 to 10.5 were used. It was observed that the maximum peak current of ferulic acid was obtained at pH 2.2 of phosphate buffer solution hence phosphate buffer with 2.2 pH was used for further analysis. The oxidation peak current of ferulic acid reaches maxima at pH 2.2 (Fig. 1a), further increase in pH of buffer solution results in the decrease of the current response (Fig. 1b).

The oxidation peak potential shift was observed and the relationship between the oxidation peak potential (E_p) and pH (2.0 to 10.0) can be represented by eqn. 1:

$$E_p/V = -0.0169\text{pH} + 0.5855 \quad (R^2 = 0.9879) \quad (1)$$

Effect of solvent: In order to obtain the maximum peak current, different solvent media *e.g.* Milli-Q water, methanol, ethanol, DMF and DMSO were used for the voltammetric study of ferulic acid. The highest peak response was observed with methanol solvent (Fig. 2) and hence was selected for further analysis of ferulic acid.

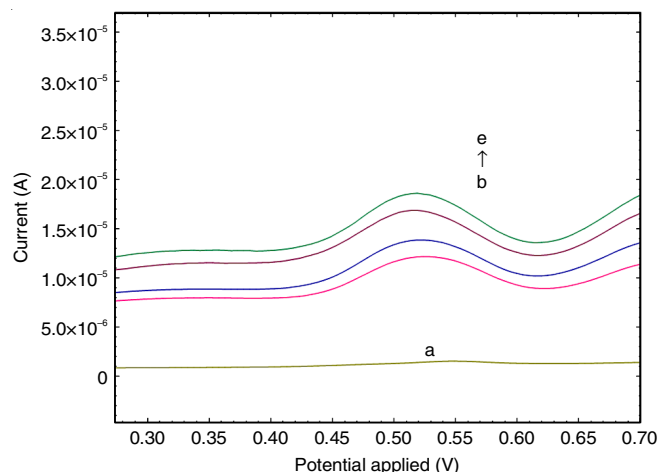


Fig. 2. Optimization of solvent (a) blank, (b) DMSO, (c) DMF, (d) ethanol and (e) methanol

Optimization of carbon mesoporous suspension (CMP) concentration: An experiment was performed to explore the effect of CMP suspension loading onto the surface of a glassy carbon electrode (GCE). It was shown that an anodic peak current response for ferulic acid was increased significantly with an increase in loading of CMP suspension ($2\text{-}12 \mu\text{L}$);

however, the maximum peak current response was obtained at 10 μL . Therefore, 10 μL was selected for further analysis of ferulic acid (Fig. 3).

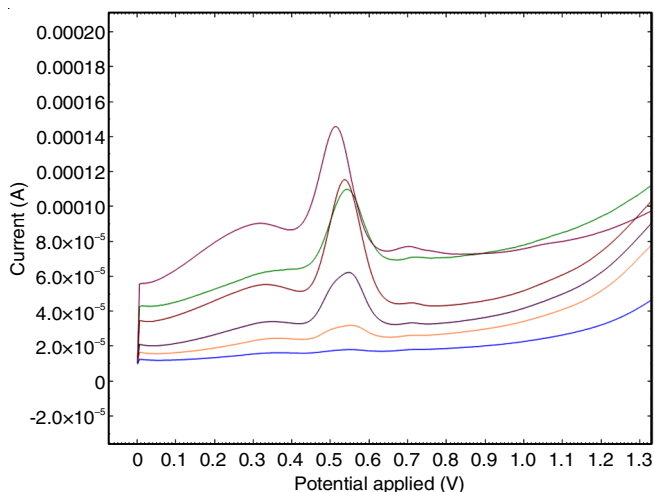


Fig. 3. Optimization of carbon mesoporous suspension

Effect of scan rate: Effect of scan rate was performed by cyclic voltammetry on the oxidation of ferulic acid at the modified (CMP/GCE) sensor. The redox behaviour of ferulic acid in the solution was investigated by the cyclic voltammetric technique. Voltammogram of 4 $\mu\text{g}/\text{mL}$ ferulic acid in phosphate buffer (pH 2.2) and 1 M KCl were recorded with different scan rate ranges from 10 to 100 mV/s (Fig. 4). Eqn. 2 expressed that anodic peak current for ferulic acid increased linearly with an increase of square root of scan rate ($v^{1/2}$) in the range of 10-100 mV s^{-1} .

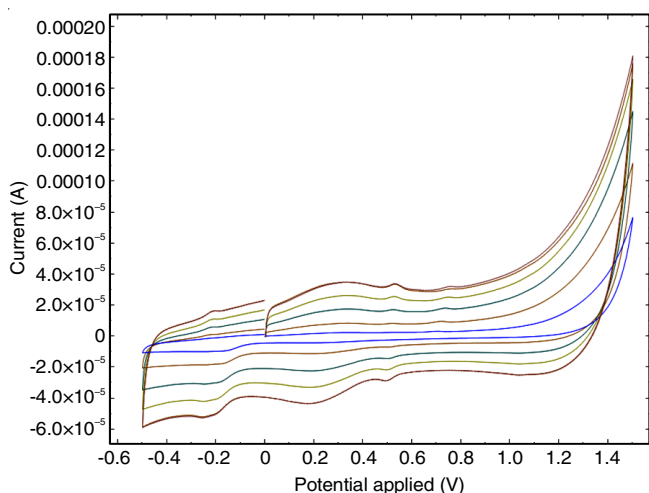


Fig. 4. Cyclic voltammogram of oxidation of ferulic acid at different scan rate range from 10 to 100 mVs^{-1}

$$I (\mu\text{A}) = 0.1159 + 0.2965 v (\text{mV s}^{-1}) \quad (R^2 = 0.9813) \quad (2)$$

When a graph is plotted between the log of peak current ($\log I$) and the log of scan rate ($\log v$), a linear relationship with using regression equation (eqn. 3) was obtained.

$$\log I (\mu\text{A}) = 0.4477 \log v (\text{mV s}^{-1}) - 0.4145 \quad (R^2 = 0.9884) \quad (3)$$

It is clearly shown from the above equation that slope is close to 0.5 results in oxidation of ferulic acid at carbon mesoporous fabricated sensor is a diffusion-controlled process [20-23].

The oxidation of ferulic acid at carbon mesoporous fabricated sensor is an irreversible process and the relationship between the anodic peak potential (E_p) of ferulic acid with Napierian logarithm of scan rate ($\ln v$) [24] can be represented by the following equation (eqn. 4):

$$E_p = E^\circ + \left(\frac{RT}{\alpha nF} \right) \ln \left(\frac{RTk^\circ}{\alpha nF} \right) + \left(\frac{RT}{\alpha nF} \right) \ln v \quad (4)$$

here, E° = formal redox potential, α = electron transfer coefficient, R = gas constant, F = Faraday constant, k° = standard heterogeneous rate constant, n = number of electrons involved.

During the oxidation of ferulic acid, anodic peak potential (E_p) linearly increases with the increase of the Napierian logarithm of scan rate ($\ln v$) in the range of 10 to 100 mV s^{-1} . This can be expressed by the following equation (eqn. 5).

$$E_p (v) = 0.03 (\ln v) + 0.422 \quad (R^2 = 0.9981) \quad (5)$$

By combining eqns. 4 and 5

$$\frac{RT}{\alpha nF} = 0.03 \quad (6)$$

where, $R = 8.314 \text{ J K}^{-1} \text{ mol}^{-1}$, $T = 298 \text{ K}$ and $F = 96,500 \text{ C}$. the value of charge transfer coefficient (α) for an irreversible oxidation process of ferulic acid is to be 0.4, which is theoretically close to 0.5. The number of electrons can be calculated from the eqn. 6 to be 2. Hence, it is confirm that two electrons are involved during the oxidation of ferulic acid at CMP/GCE.

Electrocatalytic behaviour of ferulic acid: The electrochemical behaviour of ferulic acid was studied at bare glassy carbon electrodes as well as in carbon mesoporous fabricated glassy carbon electrodes (CMP/GCE) (Fig. 5). A comparative study of the anodic peak current of ferulic acid at bare glassy carbon electrode and the modified sensor was done by square wave voltammetry (SWV) in phosphate buffer (pH 2.2) and 1.0 M KCl solution as supporting electrolyte. The obtained square wave voltammogram for bare GCE and fabricated CMP/GCE showed that due to the high conductivity and sensitivity of modified CMP/GCE, the peak current of ferulic acid as obtained from the fabricated sensor is higher than the peak current obtained from bare glassy carbon electrode, which illustrates that carbon mesoporous film enhanced the sensitivity of glassy carbon electrode. Hence, the carbon mesoporous is a relevant modifier that gives an excellent electrocatalytic activity of the sensor towards the oxidation peak of ferulic acid.

Morphological characterization of carbon mesoporous modifier: The surface morphology of carbon mesoporous was investigated by SEM analysis (Fig. 6). The carbon mesoporous shows a nearly spherical structure and when collected to form particle clusters [25].

Effective surface area: The electrocatalytic activity of fabricated sensor and bare glassy carbon electrode was comparatively studied by a cyclic voltammetric technique by using 1.0 $\text{mM K}_3[\text{Fe}(\text{CN})_6]$ as model redox probe and Randles-Savcik equation was used (eqn. 7):

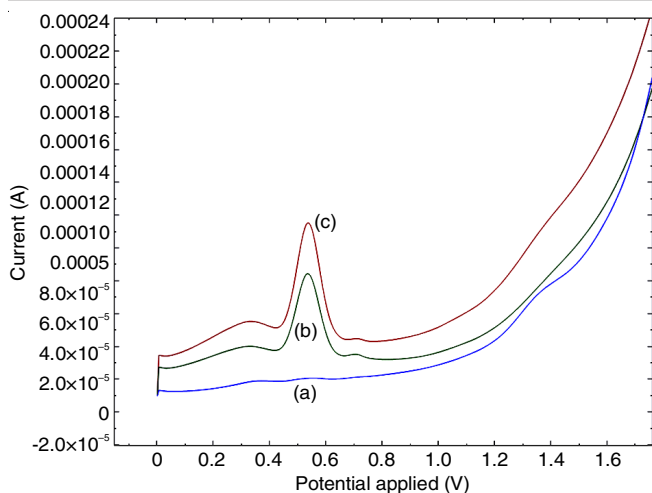


Fig. 5. Square wave voltammograms of $1 \mu\text{g mL}^{-1}$ ferulic acid in phosphate buffer (pH 2.2) (a) blank, (b) bare GCE and (c) CMP/GCE

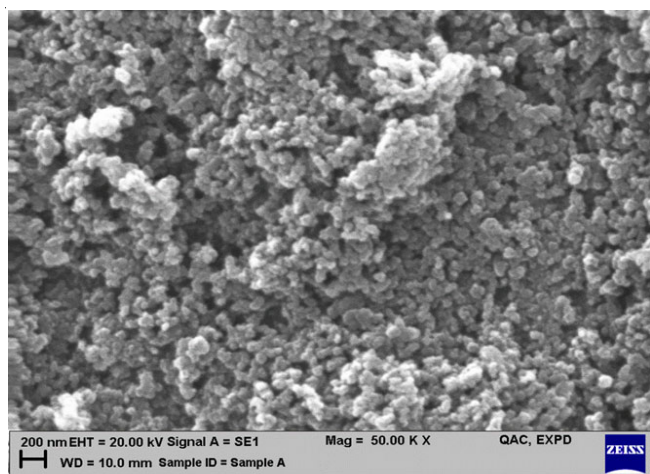


Fig. 6. SEM carbon mesoporous

$$I = (2.69 \times 10^5) A \times C \times D^{1/2} n^{3/2} v^{1/2} \quad (7)$$

where 'A' is the effective surface area in cm^2 , 'I' is the maximum current in ampere, 'C' is concentration in mol/cm^3 , 'D' is diffusion coefficient ($7.6 \times 10^{-6} \text{ cm}^2 \text{ s}^{-1}$) [22], 'v' is scan rate in V/s and 'n' is several electrons involved in electrode reaction, for $\text{K}_3[\text{Fe}(\text{CN})_6]$ $n = 1$. Cyclic voltammograms were recorded at a scan rate of 100 mV s^{-1} . A significant increment of anodic peak current was clearly seen due to carbon mesoporous modifier, which enhances the electrocatalytic activity of the sensor. A comparative study of the surface area of modified CMP/GCE as well as bare glassy carbon electrode respectively was conducted in 1.0 mM solution of $\text{K}_3[\text{Fe}(\text{CN})_6]$ containing 1.0 M KCl as supporting electrolyte (Fig. 7a). The effective surface area of fabricated carbon mesoporous glassy carbon electrode (CMP/GCE) and bare glassy carbon electrode were 0.042 cm^2 and 0.026 cm^2 , respectively. The obtained results clearly indicates that fabricated glassy carbon electrode surface area is greater than bare glassy carbon electrode.

Electrochemical impedance spectroscopic studies: The interfacial electron transfer properties of bare glassy carbon electrode and carbon mesoporous fabricated glassy carbon electrode (CMP/GCE) were carried out with electrochemical

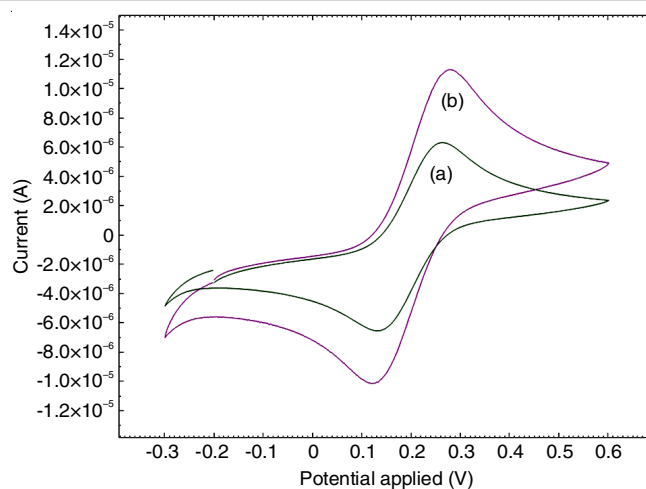


Fig. 7. Cyclic voltammograms of 1.0 mM $\text{K}_3[\text{Fe}(\text{CN})_6]$ at (a) bare GCE (b) CMP/GCE

impedance spectroscopy (EIS) [26]. The EIS of bare GCE and fabricated CMP/GCE were recorded, by using a solution of 3.0 mM $\text{K}_3[\text{Fe}(\text{CN})_6]$ in 0.1 M KCl solution as redox probe. The Nyquist plots for both bare and fabricated sensors are shown in Fig. 8. The interfacial electron transfer ability is shown by the numerical value of charge transfer resistance (R_{ct}) and is calculated by Nyquist plots as per the diameter of the semicircle. The value of charge transfer resistance (R_{ct}) for bare glassy carbon electrodes and the fabricated sensor (CMP/GCE) was $13.8 \text{ K}\Omega$ and $8.21 \text{ K}\Omega$, respectively. The obtained results shows that the R_{ct} value of bare glassy carbon electrode is much higher than the fabricated sensor (CMP/GCE). As the resistance value has an inverse relationship with the conductivity of sensor, therefore fabricated sensor (CMP/GCE) shows more conductivity than the bare glassy carbon electrode of its low R_{ct} value. The decrease in the electron transfer resistance (R_{ct}) value of fabricated glassy carbon electrodes can be associated with the large surface area and carbon mesoporous film provides an effective electron conduction pathway between the surface of the electrode and electrolyte.

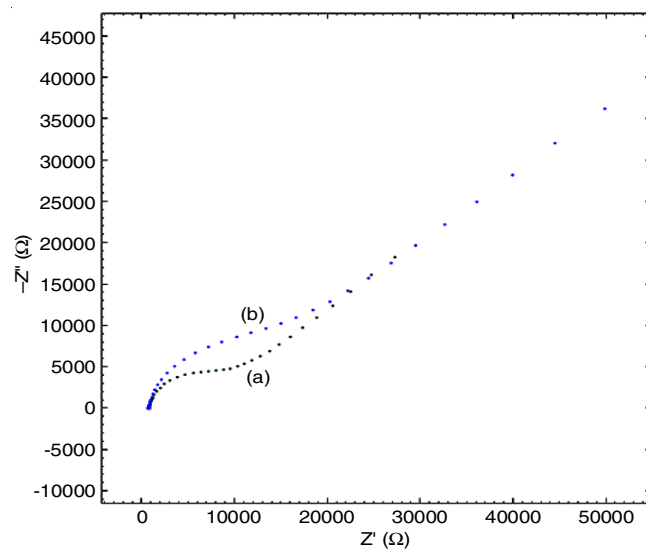


Fig. 8. Nyquist plots at (a) CMP/GCE (b) bare GCE

Validation of the proposed method

Calibration curve and limit of detection: Under the optimized experimental conditions, the electrochemical determination of ferulic acid on the CMP/GCE sensor was done by square wave voltammetry. The obtained results clearly showed that the anodic peak current of ferulic acid increased linearly with ferulic acid concentration (Fig. 9), which varies in the range from 1 to 7 $\mu\text{g/mL}$, with linear regression equation (eqn. 8) as follows:

$$I/\mu\text{A} = 0.5058 (\mu\text{g mL}^{-1}) + 0.3151; R^2 = 0.997 \quad (8)$$

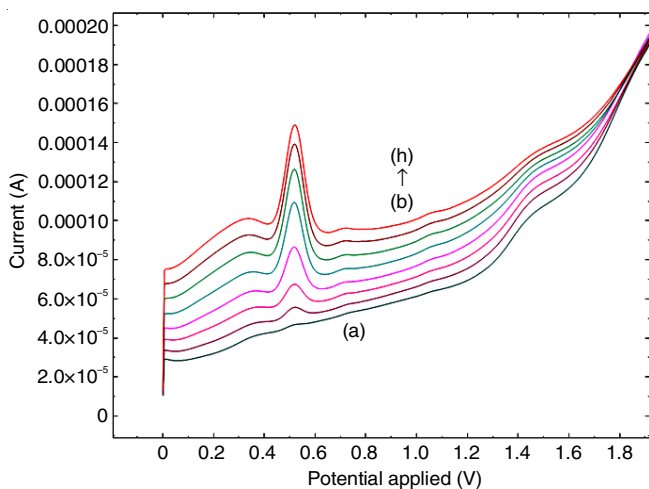


Fig. 9. Voltammograms obtained for different concentrations of ferulic acid at CMP/GCE (a) blank, (b to g) ferulic acid concentration from 1 to 7 $\mu\text{g mL}^{-1}$

The limit of detection (LOD) and limit of quantification (LOQ) were estimated by the following equations:

$$\text{LOD} = \frac{3S}{m} \quad (9)$$

$$\text{LOQ} = \frac{10S}{m} \quad (10)$$

where S = standard deviation of the intercept; m = slope of the calibration curve.

The estimated value of LOD and LOQ for ferulic acid was found to be 0.36 and 1.10 $\mu\text{g mL}^{-1}$, respectively.

Reproducibility and repeatability: The reproducibility of the fabricated CMP/GCE sensor was estimated by analyzing 6 $\mu\text{g mL}^{-1}$ ferulic acid at three different electrodes developed independently using square wave voltammetry at different intervals of time (Table-1). The square wave voltammogram of a fixed concentration of ferulic acid was recorded in replicate manner to investigate the repeatability of the fabricated (CMP/GCE) sensor. The acceptable reproducibility of the fabricated (CMP/GCE) sensor is 1.47%.

Real sample analysis: For the real sample analysis, the standard addition method was used. The prepared real sample was divided into 7 aliquots of equal volume in a separate volumetric flask of 5 mL. The first volumetric flask was diluted with methanol solvent. Then a standard containing the analyte (ferulic acid 1000 $\mu\text{g/mL}$) was added in increasing volumes (100-600 μL) to the rest of the volumetric flasks and each flask

TABLE-1
REPRODUCIBILITY DATA FOR
6 $\mu\text{g mL}^{-1}$ FERULIC ACID AT CMP/GCE

Sensors	Sensor reproducibility means current (I/ μA)	RSD (%)	Single sensor reproducibility means current (I/ μA)	RSD (%)
Sensor 1	4.52 ^a	1.35	4.52	1.35
Sensor 2	4.43 ^a	2.06		
Sensor 3	4.53 ^a	1.01		
Average	4.52 ^b	1.47		

^aMean of three replicates; ^bMean of three sensors.

was diluted with methanol. Fig. 10 shows a voltammogram of real sample analysis of ferulic acid. The anodic current response was also measured for all of the diluted solutions and plotted with concentration *versus* current response. Linear regression was obtained and the slope (m) and y-intercept (b) of the calibration curve (figure not shown), which were used to calculate the concentration of analyte (ferulic acid) in the analysis of real sample.

$$C_x = b \times \frac{C_s}{m} \times V_x \quad (11)$$

here C_x = concentration of sample, C_s = concentration of standard, m = slope of linear regression, V_x = volume of sample aliquot; b = intercept of linear regression.

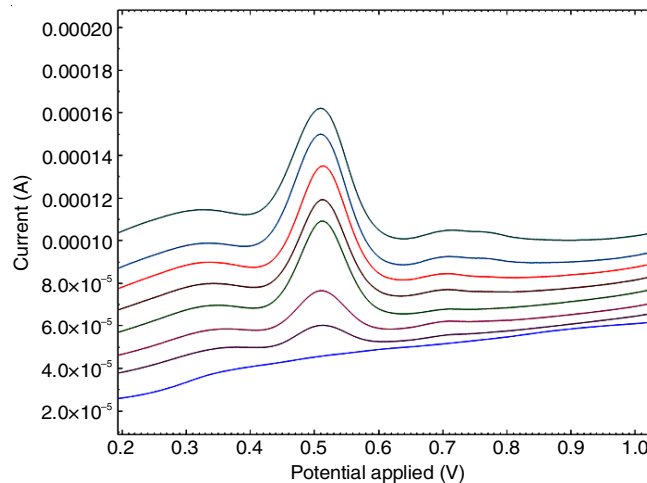


Fig. 10. Voltammogram of real sample analysis in sweet corn

Interference analysis: The selectivity of developed sensor was investigated by interference analysis with several interfering compounds such as organic compounds, inorganic ions and some other antioxidants in presence of 8 $\mu\text{g/mL}$ ferulic acid. In the presence of interferences, it was observed that change in the recovery of ferulic acid ranged from 94% to 101%, which illustrate the excellent recovery of proposed method (Table-2). The percent recovery was computed as follows [27]:

$$\text{Recovery (\%)} = \frac{\text{Current response for analyte in presence of interferent}}{\text{Current response for analyte for analyte alone}} \times 100$$

Conclusion

In this work, ferulic acid was estimated by using carbon mesoporous fabricated (CMP/GCE) sensor with square wave

TABLE-2
INTERFERENCE ANALYSIS FOR FERULIC ACID IN PRESENCE
OF DIFFERENT INTERFERENT SAMPLES AT CMP/GCE

Interferent samples	Interferent conc. (µg/mL)	Recovery (%)
Piperine	5	97
Curcumin	5	94
Inorganic ions (Na ⁺ , Ca ²⁺ , Cl ⁻ , SO ₄ ²⁻ , CO ₃ ²⁻)	7	99
Fructose	8	101
Glucose	8	100

voltammetry and cyclic voltammetric techniques. The results showed that the fabricated sensor enhances the anodic current response of ferulic acid more than the bare glassy carbon electrode. Present work is a novel, easy, fast and economical method. The developed sensor is reliable and show the satisfactory results in the real sample analysis.

ACKNOWLEDGEMENTS

The author would like to acknowledge Prof. Rajeev Jain for providing the valuable suggestions and lab facilities in School of Science (Chemistry) at Jiwaji University, Gwalior, India.

CONFLICT OF INTEREST

The authors declare that there is no conflict of interests regarding the publication of this article.

REFERENCES

- S. Ou and K.-C. Kwok, *J. Sci. Food Agric.*, **84**, 1261 (2004); <https://doi.org/10.1002/jsfa.1873>
- A. Urbaniak, M. Szlag and M. Molski, *Comput. Theor. Chem.*, **1012**, 33 (2013); <https://doi.org/10.1016/j.comptc.2013.02.018>
- J. Kanski, M. Aksenova, A. Stoyanova and D.A. Butterfield, *J. Nutr. Biochem.*, **13**, 273 (2002); [https://doi.org/10.1016/S0955-2863\(01\)00215-7](https://doi.org/10.1016/S0955-2863(01)00215-7)
- S.Y. Chung and E.T. Champagne, *Food Chem.*, **124**, 1639 (2011); <https://doi.org/10.1016/j.foodchem.2010.07.086>
- A. Murakami, Y. Nakamura, K. Koshimizu, D. Takahashi, T. Tsuno, K. Matsumoto, K. Hagihara, H. Taniguchi, E. Nomura, A. Hosoda, Y. Maruta, H.W. Kim, K. Kawabata and H. Ohigashi, *Cancer Lett.*, **180**, 121 (2002); [https://doi.org/10.1016/S0304-3835\(01\)00858-8](https://doi.org/10.1016/S0304-3835(01)00858-8)
- A.J. Blasco, A. González Crevillén, M.C. González and A. Escarpa, *Electroanalysis*, **19**, 2275 (2007); <https://doi.org/10.1002/elan.200704004>
- E. Graf, *Free Radic. Biol. Med.*, **13**, 435 (1992); [https://doi.org/10.1016/0891-5849\(92\)90184-I](https://doi.org/10.1016/0891-5849(92)90184-I)
- M.A. Alam, C. Sernia and L. Brown, *J. Cardiovasc. Pharmacol.*, **61**, 240 (2013); <https://doi.org/10.1097/FJC.0b013e31827cb600>
- W. Sompong, A. Meeprom, H. Cheng and S. Adisakwattana, *Molecules*, **18**, 13886 (2013); <https://doi.org/10.3390/molecules181113886>
- R. Sultana, *Biochim. Biophys. Acta*, **1822**, 748 (2012); <https://doi.org/10.1016/j.bbadis.2011.10.015>
- H. Taniguchi, A. Hosoda, T. Tsuno, Y. Maruta and E. Nomura, *Anticancer Res.*, **19**, 3757 (1999).
- S. Pal, S. Maity, S. Sardar, S. Begum, R. Dalui, H. Parvej, K. Bera, A. Pradhan, N. Sepay, S. Paul and U.C. Halder, *J. Chem. Sci.*, **132**, 103 (2020); <https://doi.org/10.1007/s12039-020-01796-z>
- R.K. Harwansh, P.K. Mukherjee, S. Bahadur and R. Biswas, *Life Sci.*, **141**, 202 (2015); <https://doi.org/10.1016/j.lfs.2015.10.001>
- W.D. Cai, J. Zhu, L.X. Wu, Z.R. Qiao, L. Li and J.K. Yan, *Food Chem.*, **300**, 125221 (2019); <https://doi.org/10.1016/j.foodchem.2019.125221>
- A. Amic, Z. Markovic, J.M. Dimitric Markovic, D. Milenkovic and V. Stepanic, *Phytochemistry*, **170**, 112218 (2020); <https://doi.org/10.1016/j.phytochem.2019.112218>
- S. Palani Swamy and V. Govindaswamy, *J. Funct. Foods*, **17**, 657 (2015); <https://doi.org/10.1016/j.jff.2015.06.013>
- Z. Xia, Y. Zhang, Q. Li, H. Du, G. Gui and G. Zhao, *Int. J. Electrochem. Sci.*, **15**, 559 (2020); <https://doi.org/10.20964/2020.01.49>
- X. Li, G. Liu, Y. Tu, J. Li and S. Yan, *Food Chem.*, **278**, 502 (2019); <https://doi.org/10.1016/j.foodchem.2018.10.086>
- S. Irshad and S. Khatoon, *J. Planar Chromatogr. Mod. TLC*, **31**, 429 (2018); <https://doi.org/10.1556/1006.2018.31.6.2>
- C.M.A. Brett and A.M.O. Brett, *Electrochim. Acta*, **39**, 853 (1993).
- P.T. Kissinger, W.H. Heineman, *Laboratory Techniques in Electroanalytical Chemistry*, Second Edition, Marcel Dekker, INC.: New York and Basel (1996).
- A.J. Bard and L.R. Faulkner, *Electrochemical Methods: Fundamentals and Applications*, Edn.: 2, Wiley: New York (1980).
- R. Jain, R. Mishra and A. Dwivedi, *J. Sci. Ind. Res. (India)*, **68**, 945 (2008).
- A. Sinha, R. Dhanjai and R. Jain, *Mater. Res. Bull.*, **65**, 307 (2015); <https://doi.org/10.1016/j.materresbull.2015.02.001>
- M.A. Zulkifli, A. Afandi and A.T.M. Din, *AIP Conf. Proc.*, **2124**, 020026 (2019); <https://doi.org/10.1063/1.5117086>
- K. Singh, N. Jadon and R. Jain, *Colloids Surf. B Biointerfaces*, **166**, 72 (2018); <https://doi.org/10.1016/j.colsurfb.2018.02.057>
- R. Jain and A. Verma, *Int. J. Electrochem. Sci.*, **12**, 3459 (2017); <https://doi.org/10.20964/2017.04.29>